

# Collective Qubit States and the Tavis-Cummings Model in Circuit QED

J. M. Fink,<sup>1</sup> R. Bianchetti,<sup>1</sup> M. Baur,<sup>1</sup> M. Göppl,<sup>1</sup> L. Steffen,<sup>1</sup> S. Filipp,<sup>1</sup> P. J. Leek,<sup>1</sup> A. Blais,<sup>2</sup> and A. Wallraff<sup>1</sup>

<sup>1</sup>*Department of Physics, ETH Zurich, CH-8093, Zurich, Switzerland.*

<sup>2</sup>*Département de Physique, Université de Sherbrooke, Sherbrooke, Québec J1K 2R1, Canada.*

(Dated: June 21, 2024)

The collective dipole interaction of  $N$  individual atoms, spins or qubits with a photon stored in a single mode of a cavity field is described by the Tavis-Cummings model [1]. This model predicts an enhancement of the collective  $N$ -atom/photon dipole coupling strength  $g_N$  by a factor of  $\sqrt{N}$  over the individual atom/photon coupling strength  $g$ . This effect was investigated in atomic physics experiments for small average atom numbers  $\bar{N}$  [2, 3, 4, 5] and more recently also for very large  $\bar{N}$  [6, 7, 8]. In these experiments fluctuations in the atom positions with respect to the cavity mode lead to substantial fluctuations both in  $\bar{N}$  and in  $g$  which become particularly relevant for small  $N$ . Here we present an ideal realization of the Tavis-Cummings model avoiding both atom number and coupling fluctuations by embedding a discrete number of fully controllable superconducting qubits at fixed positions into a transmission line resonator [9, 10]. Measuring the vacuum Rabi mode splitting with one, two and three qubits strongly coupled to the cavity field, we explore both bright and dark collective multi-qubits states and observe the discrete  $\sqrt{N}$  scaling of the coupling strength. Our experiments demonstrate a novel approach to explore collective states, such as the  $W$ -state [11], in a fully globally and locally controllable quantum system. Our scalable approach is interesting both for solid-state quantum information processing and for fundamental multi-atom quantum optics experiments.

In the early 1950's Dicke realized that under certain conditions a gas of radiating molecules shows the collective behavior of a single quantum system [12]. The idealized situation in which  $N$  two-level systems with identical dipole coupling are resonantly interacting with a single mode of the electromagnetic field was analyzed by Tavis and Cummings [1]. This model predicts the collective  $N$ -atom interaction strength to be  $g_N = g_j \sqrt{N}$ , where  $g_j$  is the dipole coupling strength of each individual atom  $j$ . In fact, in first cavity QED experiments the normal mode splitting, observable in the cavity transmission spectrum [13, 14], was demonstrated with on average  $\bar{N} > 1$  atoms in optical [15, 16] and microwave [2] cavities to overcome the relatively weak dipole coupling  $g_j$ . The  $\sqrt{N}$  scaling has been observed in the regime of a small mean number of atoms  $\bar{N}$  with dilute atomic beams [2, 3, 4] and fountains [5] crossing a high-finesse cavity. In these experiments, spatial variations of the atom positions and Poissonian fluctuations in the atom number inherent to an atomic beam [3, 14, 17] are unavoidable. In a different limit where the cavity was populated with a very large number of ultra-cold  $^{87}\text{Rb}$  atoms [6] and more recently with Bose-Einstein condensates [7, 8] the  $\sqrt{N}$  nonlinearity was also demonstrated. However, the number of interacting atoms is typically only known to about  $\sim 10\%$  [7].

Here we present an experiment in which the Tavis-Cummings model is studied for a discrete set of artificial atoms at fixed positions and with virtually identical couplings to a resonant cavity mode. The investigated situation is sketched in Fig. 1 a, depicting an optical analog where three two-state atoms are deterministically positioned at electric field antinodes of a cavity mode

where the coupling is maximum. In our circuit QED [9, 10] realization of this configuration (Fig. 1 b), three transmon-type [18] superconducting qubits are embedded in a microwave resonator which contains a quantized radiation field. The cavity is realized as a coplanar waveguide resonator with a first harmonic full wavelength resonance frequency of  $\omega_r/2\pi = 6.729$  GHz and a photon decay rate of  $\kappa/2\pi = 6.8$  MHz. The qubits are positioned at the antinodes of the first harmonic standing wave electric field. The transition frequency between

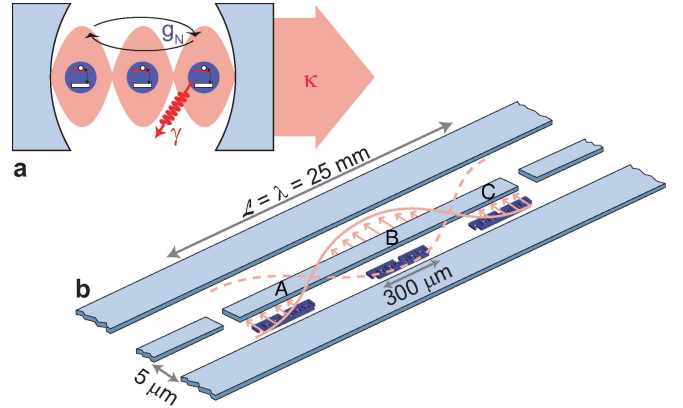


Fig. 1: **Schematic of the experimental set-up.** a, Optical analog. Three two-state atoms are identically coupled to a cavity mode with photon decay rate  $\kappa$ , energy relaxation rate  $\gamma$  and collective coupling strength  $g_N$ . b, Schematic of the investigated system. The coplanar waveguide resonator is shown in light blue, the transmon qubits A, B and C in violet and the first harmonic of the standing wave electric field in red.

ground  $|g\rangle$  and first excited state  $|e\rangle$  of qubit  $j$ , approximately given by  $\omega_j/2\pi \approx \sqrt{8E_{C_j}E_{J_j}(\Phi_j)} - E_{C_j}$ , is controllable through the flux dependent Josephson energy  $E_{J_j}(\Phi_j) = E_{J_{\max_j}}|\cos(\pi\Phi_j/\Phi_0)|$  [18]. Here  $E_{C_j}$  is the single electron charging energy,  $E_{J_{\max_j}}$  the maximum Josephson energy at flux  $\Phi_j = 0$  and  $\Phi_0$  the magnetic flux quantum. Independent flux control of each qubit is achieved by applying magnetic fields with three external miniature current biased coils (Fig. 2 a) where we take into account all cross-couplings by inverting the full coupling matrix. Optical images of the investigated sample are depicted in Fig. 2 b and c. The resonator was fabricated employing optical lithography and Aluminum evaporation techniques on a Sapphire substrate. All qubits were fabricated with electron beam lithography and standard  $Al/AlO_x/Al$  shadow evaporation techniques. Table I states the individual qubit parameters obtained from spectroscopic measurements.

The physics of our system is described by the Tavis-Cummings Hamiltonian [1]

$$\hat{\mathcal{H}}_{TC} = \hbar\omega_r\hat{a}^\dagger\hat{a} + \sum_{j=1}^N \left( \frac{\hbar}{2}\omega_j\hat{\sigma}_j^z + \hbar g_j(\hat{a}^\dagger\hat{\sigma}_j^- + \hat{\sigma}_j^+\hat{a}) \right), \quad (1)$$

where  $g_j$  is the coupling strength between the field and qubit  $j$ .  $\hat{a}^\dagger$  and  $\hat{a}$  are the creation and annihilation operators acting on the photon number states of the field,  $\hat{\sigma}_j^+$ ,  $\hat{\sigma}_j^-$  are the corresponding operators acting on the qubit  $j$  and  $\hat{\sigma}_j^z$  is a Pauli operator. The ground state  $|g, g, g\rangle \otimes |0\rangle$  of the three-qubit/cavity system is prepared by cooling the microchip to a temperature of 20 mK in a dilution refrigerator.

First we investigate the resonant coupling of the  $|g\rangle$  to  $|e\rangle$  transition of qubit A to the first harmonic mode of the resonator. We measure the anti-crossing between qubit A ( $\nu_A$ ) and the cavity ( $\nu_r$ ) by populating the resonator with much less than a photon on average. We record the resulting transmission spectrum  $T$  versus magnetic flux  $\Phi_A$  controlled detuning of qubit A (Fig. 3 a). Qubits B and C remain maximally detuned from the resonator at  $\Phi_B = \Phi_C = \Phi_0/2$  where they do not affect the measurement performed with qubit A. At finite detuning (left hand side of Fig. 3a) we observe a shift of the resonator spectrum which increases with decreasing detuning due to the dispersive interaction with qubit A.

Qubit $j$	$E_{C_j}$ (MHz)	$E_{J_{\max_j}}$ (GHz)	$g_j/2\pi$ (MHz)
A	148	409	83.7
B	149	415	-85.4
C	153	392	84.9

Tab. I: **Qubit and qubit-resonator coupling parameters.** The single electron charging energy  $E_{C_j}$ , the maximum Josephson energy  $E_{J_{\max_j}}$  extracted from spectroscopic measurements and the coupling strengths  $g_j$  obtained from resonator transmission measurements for qubits A, B and C.

On resonance ( $\omega_j = \omega_r$ ) and in the presence of just one two level system ( $N = 1$ ), Eq. (1) reduces to the Jaynes-Cummings Hamiltonian [19]. The eigenstates of this system in the presence of just one excitation  $n = 1$  are the symmetric and anti-symmetric qubit-photon superpositions  $|N, n \pm\rangle = |1, 1 \pm\rangle = 1/\sqrt{2} (|g, 1\rangle \pm |e, 0\rangle)$  (Fig. 4 a) where the excitation is equally shared between qubit and photon. Accordingly, we observe a clean vacuum Rabi mode splitting spectrum formed by the states  $|1, 1 \pm\rangle$  (Fig. 3 b). From analogous measurements performed on qubits B and C (not shown) we obtain the single qubit coupling constants  $g_j$  listed in table I. The coupling strengths are virtually identical with a scatter of only a few MHz. The strong coupling of an individual

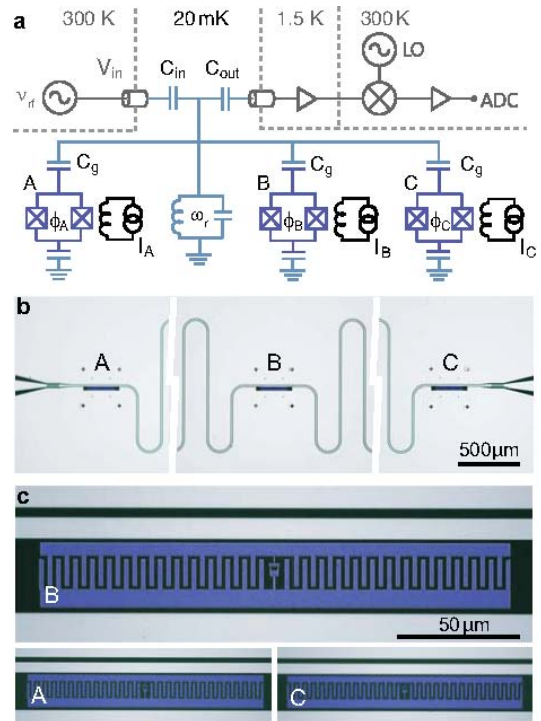


Fig. 2: **Circuit diagram and false color optical images of the sample.** a, Simplified electrical circuit diagram of the experimental setup. The waveguide resonator operated at a temperature of 20 mK, indicated as LC oscillator with frequency  $\omega_r$ , is coupled to input and output leads with the capacitors  $C_{in}$  and  $C_{out}$ . Qubits A, B and C are controlled with external current biased coils ( $I_{A,B,C}$ ) and coupled to the resonator via identical capacitors  $C_g$ . A transmission measurement is performed by applying a measurement tone  $\nu_{rf}$  to the input port of the resonator, amplifying the transmitted signal and digitizing it with an analog-to-digital converter (ADC) after down-conversion with a local oscillator (LO) in a heterodyne detection scheme. b, The coplanar microwave resonator is shown truncated in gray (substrate in dark green) and the locations of qubits A, B and C are indicated. c, Top, magnified view of transmon qubit B (violet) embedded between ground plane and center conductor of the resonator. Bottom, qubits A and C, of the same dimensions as qubit B, are shown at reduced scale.

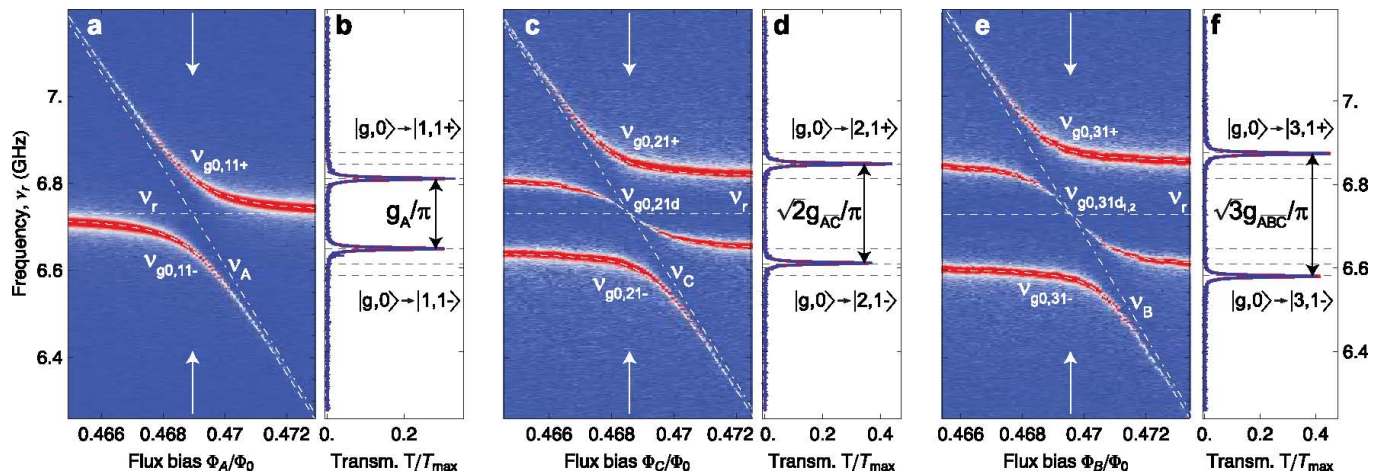


Fig. 3: **Vacuum Rabi mode splitting with one, two and three qubits.** a, Measured resonator transmission spectrum  $T$  (blue, low and red, high transmission) versus normalized external flux bias  $\Phi_A/\Phi_0$  of qubit A. Dash-dotted white lines indicate bare resonator  $\nu_r$  and qubit  $\nu_A$  frequencies and dashed white lines are calculated transition frequencies  $\nu_{g_0, Nn\pm}$  between  $|g, 0\rangle$  and  $|N, n\pm\rangle$ . b, Resonator transmission  $T/T_{\max}$  at degeneracy normalized to the maximum resonator transmission  $T_{\max}$  measured at  $\Phi_{A,B,C} = \Phi_0/2$  (not shown), as indicated with arrows in a. Red line is a fit to two Lorentzians. c, Resonator transmission spectrum  $T/T_{\max}$  versus external flux bias  $\Phi_C/\Phi_0$  of qubit C with qubit A degenerate with the resonator ( $\nu_A = \nu_r$ ). d, Transmission spectrum  $T/T_{\max}$  at flux as indicated in c. e, Transmission spectrum versus flux  $\Phi_B/\Phi_0$  with both qubits A and C at degeneracy ( $\nu_A = \nu_C = \nu_r$ ). The white dashed line at frequency  $\nu_{g_0, 31d_{1,2}} = \nu_r$  indicates the dark state occurring at degeneracy. f, Transmission spectrum  $T/T_{\max}$  at flux as indicated in e.

photon and an individual two-level system has been observed in a wealth of different realizations of cavity QED both spectroscopically [9, 20, 21] and in time-resolved experiments [22, 23]. The regime of multiple excitations  $n$  which proves field quantization in these systems has been reported both in the time resolved results cited above and more recently also in spectroscopic measurements [24, 25, 26].

In a next step, we maintain qubit A at degeneracy

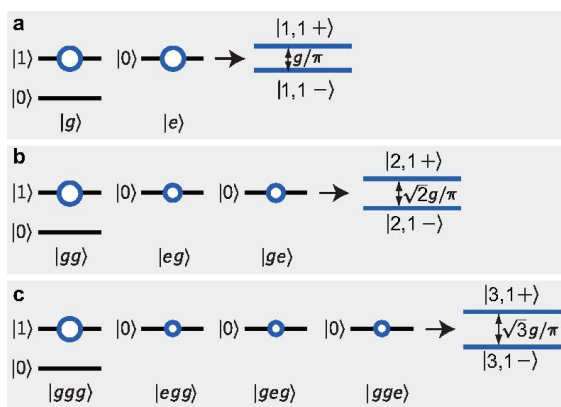


Fig. 4: **Level diagram of multiple two-level atoms resonantly coupled to a single photon.** a, One b, two and c, three qubits resonantly coupled to a quantized cavity mode. Bare energy levels of the qubits  $|g\rangle$ ,  $|e\rangle$  and the cavity  $|0\rangle$ ,  $|1\rangle$  are shown in black. The bright dressed energy levels  $|N, n\pm\rangle$  are illustrated in blue. The area of the circles indicates the population of the bare states in the eigenstates  $|N, n\pm\rangle$ .

( $\nu_A = \nu_r$ ), where we observed the one-photon one-qubit doublet (see left of Fig. 3c). Qubit B remains far detuned ( $\Phi_B = \Phi_0/2$ ) for the entire measurement. Qubit C is then tuned through the already coupled states from lower to higher values of flux  $\Phi_C$ . In this case, the doublet states  $|1, 1\pm\rangle$  of qubit A are found to be dispersively shifted due to non-resonant interaction with qubit C (Fig. 3c). When both qubits and the resonator are exactly in resonance, the transmission spectrum  $T$  (Fig. 3d) shows only two distinct maxima corresponding to the doublet  $|2, 1\pm\rangle = 1/\sqrt{2} |g, g\rangle \otimes |1\rangle \pm 1/2 (|e, g\rangle + |g, e\rangle) \otimes |1\rangle$  with eigenenergies  $\hbar(\omega_r \pm g_2)$ . Here a single excitation is shared between one photon, with probability 1/2, and two qubits, with probability 1/4 each (Fig. 4b). Both states have a photonic component and can be excited from the ground state  $|g, g, g\rangle \otimes |0\rangle$  by irradiating the cavity with light. These are thus referred to as bright states. In general we expect  $N + n = 3$  eigenstates for two qubits and one photon. The third state  $|2, 1d\rangle = 1/\sqrt{2} (|e, g\rangle - |g, e\rangle) \otimes |0\rangle$  with energy  $\hbar\omega_r$  at degeneracy has no matrix element with a cavity excitation and is referred to as a dark state. Accordingly we observe no visible population in the transmission spectrum at frequency  $\nu_r$  at degeneracy. In this regime the two qubits behave like one effective spin with the predicted coupling strength  $g_2 = \sqrt{2}g_{AC}$  with  $g_{AC} = (g_A + g_C)/2$  which is indicated by dashed black lines in Fig. 3d. This prediction is in good agreement with our transmission measurement.

Following the same procedure, we then flux tune qubit B through the already resonantly coupled states

of qubits A, C and the cavity ( $\nu_A = \nu_C = \nu_r$ ), (Fig. 3 e). We observe the energies of three out of  $N + n = 4$  eigenstates, one of which is dark, for a range of flux values  $\Phi_B$ . Starting with the dark state  $|2, 1d\rangle$  at frequency  $\nu_r$  and the doublet  $|2, 1\pm\rangle$  (left part of Fig. 3 e), the presence of qubit B dresses these states and shifts the doublet  $|2, 1\pm\rangle$  down in frequency. Again one of these states turns dark as it approaches degeneracy where it is entirely mixed with qubit B. At degeneracy we identify two bright doublet states  $|3, 1\pm\rangle = 1/\sqrt{2} |g, g, g\rangle \otimes |1\rangle \pm 1/\sqrt{6} (|e, g, g\rangle - |g, e, g\rangle + |g, g, e\rangle) \otimes |0\rangle$  (Fig. 4 c). The symmetry of these states is determined by the sign of the coupling constants  $g_A \approx -g_B \approx g_C$  set by the chosen positions of the qubits in the cavity field. The part of the states  $|3, 1\pm\rangle$  carrying the atomic excitation is a so called  $W$ -state, in which a single excitation is equally shared among all  $N$  qubits [11]. Both  $|3, 1\pm\rangle$  states are clearly visible in the transmission spectrum shown in Fig. 3 f.

In addition, there are two dark states  $|3, 1d_1\rangle = 1/\sqrt{2}(|e, g, g\rangle - |g, g, e\rangle) \otimes |0\rangle$  and  $|3, 1d_2\rangle = 1/\sqrt{2}(|g, e, g\rangle + |g, g, e\rangle) \otimes |0\rangle$  which do not lead to resonances in the transmission spectrum at degeneracy. In general all  $N + n - 2$  dark states are degenerate at energy  $\hbar\omega_r$ . Again, the observed transmission peak frequencies are in agreement with the calculated splitting of the doublet  $g_3 = \sqrt{3}g_{\overline{ABC}}$  (dashed black lines in Fig. 3 f). Also at finite detunings the measured energies of all bright states are in excellent agreement with the predictions based on the Tavis-Cummings model (dashed white lines in Fig. 3 a,c,e) using the measured qubit and resonator parameters. We have also performed analogous measurements of all twelve one, two and three qubit anti-crossings (nine are not shown) and find equally good agreement with the model.

In Fig. 5 the measured coupling strengths for one, two and three qubits at degeneracy (blue dots) are plotted vs.  $N$ . Excellent agreement with the expected collective interaction strength  $g_N = \sqrt{N}g_{\overline{ABC}}$  (red line) is found without any fit parameters and  $g_{\overline{ABC}} = 84.7$  MHz.

Our spectroscopic measurements clearly demonstrate the collective interaction of a discrete number of quantum two-state systems mediated by an individual photon. All results are in good agreement with the predictions of the basic Tavis-Cummings model in the absence of any number, position or coupling fluctuations. Our experiments may enable novel investigations of super- and sub-radiant as well as squeezed collective spin states of artificial atoms. The controlled generation of Dicke states [27] and entanglement generation via collective interactions [28, 29], not relying on individual qubit operations, could be used for quantum state engineering and an implementation of Heisenberg limited spectroscopy [30] in the solid state.

We thank T. Esslinger and A. Imamoglu for discussions. This work was supported by SNF grant no. 200021-

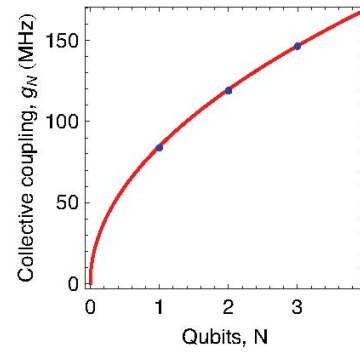


Fig. 5: **Scaling of the collective dipole coupling strength.** Measured (blue dots) and theoretical (red line) coupling constant.

111899 and ETHZ. P. J. L. was supported by the EU with a MC-EIF. A. B. was supported by NSERC, CIFAR and FQRNT.

- 
- [1] Tavis, M. and Cummings, F. W. Exact solution for an  $N$ -molecule-radiation-field Hamiltonian. *Phys. Rev.* **170**, 379–384 (1968).
  - [2] Bernardot, F., Nussenzveig, P., Brune, M., Raimond, J. M., and Haroche, S. Vacuum Rabi splitting observed on a microscopic atomic sample in a microwave cavity. *Europhys. Lett.* **17**, 33–38 (1992).
  - [3] Childs, J. J., An, K., Otteson, M. S., Dasari, R. R., and Feld, M. S. Normal-mode line shapes for atoms in standing-wave optical resonators. *Phys. Rev. Lett.* **77**, 2901 (1996).
  - [4] Thompson, R. J., Turchette, Q. A., Carnal, O., and Kimble, H. J. Nonlinear spectroscopy in the strong-coupling regime of cavity QED. *Phys. Rev. A* **57**, 3084 (1998).
  - [5] Münstermann, P., Fischer, T., Maunz, P., Pinkse, P. W. H., and Rempe, G. Observation of cavity-mediated long-range light forces between strongly coupled atoms. *Phys. Rev. Lett.* **84**, 4068 (2000).
  - [6] Tuchman, A. K., Long, R., Vrijsen, G., Boudet, J., Lee, J., and Kasevich, M. A. Normal-mode splitting with large collective cooperativity. *Phys. Rev. A* **74**, 053821–4 (2006).
  - [7] Brennecke, F., Donner, T., Ritter, S., Bourdel, T., Kohl, M., and Esslinger, T. Cavity QED with a Bose-Einstein condensate. *Nature* **450**, 268–271 (2007).
  - [8] Colombe, Y., Steinmetz, T., Dubois, G., Linke, F., Hunger, D., and Reichel, J. Strong atom-field coupling for Bose-Einstein condensates in an optical cavity on a chip. *Nature* **450**, 272–276 (2007).
  - [9] Wallraff, A., Schuster, D. I., Blais, A., Frunzio, L., Huang, R. S., Majer, J., Kumar, S., Girvin, S. M., and Schoelkopf, R. J. Strong coupling of a single photon to a superconducting qubit using circuit quantum electrodynamics. *Nature* **431**, 162–167 (2004).
  - [10] Schoelkopf, R. and Girvin, S. Wiring up quantum systems. *Nature* **451**, 664 (2008).
  - [11] Dür, W. and Vidal, G. and Cirac, J. I. Three qubits can

- be entangled in two inequivalent ways. *Phys. Rev. A* **62**, 062314 (2000).
- [12] Dicke, R. H. Coherence in spontaneous radiation processes. *Phys. Rev.* **93**, 99 (1954).
- [13] Agarwal, G. S. Vacuum-field Rabi splittings in microwave absorption by Rydberg atoms in a cavity. *Phys. Rev. Lett.* **53**, 1732–1734 (1984).
- [14] Leslie, S., Shenvi, N., Brown, K. R., Stamper-Kurn, D. M., and Whaley, K. B. Transmission spectrum of an optical cavity containing  $N$  atoms. *Phys. Rev. A* **69**, 043805 (2004).
- [15] Raizen, M. G., Thompson, R. J., Brecha, R. J., Kimble, H. J., and Carmichael, H. J. Normal-mode splitting and linewidth averaging for two-state atoms in an optical cavity. *Phys. Rev. Lett.* **63**, 240–243 (1989).
- [16] Zhu, Y., Gauthier, D. J., Morin, S. E., Wu, Q., Carmichael, H. J., and Mossberg, T. W. Vacuum Rabi splitting as a feature of linear-dispersion theory: Analysis and experimental observations. *Phys. Rev. Lett.* **64**, 2499–2502 (1990).
- [17] Carmichael, H. J. and Sanders, B. C. Multiatom effects in cavity QED with atomic beams. *Phys. Rev. A* **60**, 2497 (1999).
- [18] Koch, J., Yu, T. M., Gambetta, J., Houck, A. A., Schuster, D. I., Majer, J., Blais, A., Devoret, M. H., Girvin, S. M., and Schoelkopf, R. J. Charge-insensitive qubit design derived from the Cooper pair box. *Phys. Rev. A* **76**, 042319 (2007).
- [19] Jaynes, E. and Cummings, F. Comparison of quantum and semiclassical radiation theories with application to the beam maser. *Proceedings of the IEEE* **51**, 89–109 (1963).
- [20] Boca, A., Miller, R., Birnbaum, K. M., Boozer, A. D., McKeever, J., and Kimble, H. J. Observation of the vacuum Rabi spectrum for one trapped atom. *Phys. Rev. Lett.* **93**, 233603 (2004).
- [21] Khitrova, G., Gibbs, H. M., Kira, M., Koch, S. W., and Scherer, A. Vacuum Rabi splitting in semiconductors. *Nat. Phys.* **2**, 81–90 (2006).
- [22] Brune, M., Schmidt-Kaler, F., Maali, A., Dreyer, J., Hänggler, E., Raimond, J. M., and Haroche, S. Quantum Rabi oscillation: A direct test of field quantization in a cavity. *Phys. Rev. Lett.* **76**, 1800–1803 (1996).
- [23] Hofheinz, M., Weig, E. M., Ansmann, M., Bialczak, R. C., Lucero, E., Neeley, M., O’Connell, A. D., Wang, H., Martinis, J. M., and Cleland, A. N. Generation of Fock states in a superconducting quantum circuit. *Nature* **454**, 310–314 (2008).
- [24] Schuster, I., Kubanek, A., Fuhrmanek, A., Puppe, T., Pinkse, P. W. H., Murr, K., and Rempe, G. Nonlinear spectroscopy of photons bound to one atom. *Nat. Phys.* **4**, 382–385 (2008).
- [25] Fink, J. M., Göppl, M., Baur, M., Bianchetti, R., Leek, P. J., Blais, A., and Wallraff, A. Climbing the Jaynes-Cummings ladder and observing its nonlinearity in a cavity QED system. *Nature* **454**, 315–318 (2008).
- [26] Bishop, L. S., Chow, J. M., Koch, Jens, Houck, A. A., Devoret, M. H., Thuneberg, E., Girvin, S. M., Schoelkopf, R. J. Nonlinear response of the vacuum Rabi resonance. *arXiv:0807.2882v1* (2008).
- [27] Stockton, J. K., van Handel, R., and Mabuchi, H. Deterministic Dicke-state preparation with continuous measurement and control. *Phys. Rev. A* **70**, 022106 (2004).
- [28] Tessier, T., Deutsch, I. H., Delgado, A., and Fuentes-Guridi, I. Entanglement sharing in the two-atom Tavis-Cummings model. *Phys. Rev. A* **68**, 062316 (2003).
- [29] Retzker, A., Solano, E., and Reznik, B. Tavis-Cummings model and collective multiqubit entanglement in trapped ions. *Phys. Rev. A* **75**, 022312–6 (2007).
- [30] Leibfried, D., Barrett, M. D., Schaetz, T., Britton, J., Chiaverini, J., Itano, W. M., Jost, J. D., Langer, C., and Wineland, D. J. Toward Heisenberg-limited spectroscopy with multiparticle entangled states. *Science* **304**, 1476–1478 (2004).